Dual Robust Controller Design for High Power AC Servo drive

Stone Cheng†, Yuan-Yong Huang, Hsin-Hung Chou

†Department of Mechanical Engineering, National Chiao-Tung University, Hsinchu, Taiwan, ROC

Mechatronics Control Dept., Intelligent Machinery Technology Div., MSL/ITRI, Hsinchu, Taiwan, ROC

***Abstract*- High power AC motors have a highly interacting multivariable control structure, and it is difficult to design high dynamic performance AC drive with traditional PID-like controller for high power AC servo motor. This paper presents analysis, design and simulation of velocity loop dual robust controller for 11kw permanent magnetic synchronous motor (PMSM) in the AC servo system. By combining PDFF-MA and H^∞ control algorithms with its own capability of achieving good performance criteria such as dynamic reference tracking and load torque disturbance rejection,**

The PDFF-MA controller is designed and analyzed in the forward loop to provide low frequency stiffness and overcome low-frequency disturbances like friction. To compensate the system response, moving average(MA) error filter is added. While in the feedback loop, H^∞ controller is designed to meet system robust stability with the existence of external disturbance and model perturbations. The proposed PDFF-MA and H^∞ controllers are designed based on the transfer function of the poly-phase synchronous machine in the synchronous reference frame at field orientation control (FOC). The parameter variations, load changes, and set-point variations of synchronous machine are taking into consideration to study the dynamic performance.

Keywords: AC servo motor, PDFF-MA controller, H^∞ feedback control,

I. Introduction

The AC servo drive plays an important role in industrial motion control applications including machine tools, factory automation and robotics in the low-to-medium power range. Several situations encountered in these applications: 1) Load inertia and friction variation during operation as the payload changes. 2) The presence of a tensional resonance of the mechanical system limited the System bandwidth. 3) In AC servo motors, higher torque ripple and coupled dynamics with magnetic flux caused the nonlinearities in torque response and torque transients. 4) During these applications, the set-point tracking capability in both dynamic and steady-state conditions and the load torque disturbance rejection capability are varying. Several control techniques [1-7] have been developed to overcome these issues. Derived from generalized PID controller, the PDFF controller is allowing the user to eliminate overshoot and provide much more DC stiffness than PI by properly choosing the controller parameters and is less sensitive to plant parameter variations, and its disturbance rejection characteristics are much better than that of the PI controller. Along with PDFF controller, H^∞ control theory is one of the successful algorithms for robust control problem in AC servo drive to provide better tolerance to disturbance and modeling uncertainties. In this paper, the H^∞ design procedure[5,9,10] is proposed and consists three main stages: 1) using weighting matrices W_1 and W_2 to shape the singular values of the nominal plant follows the elementary open-loop shaping principles; 2) the normalized coprime factor H^∞ problem is used to find a robust central controller stabilizing this shaped plant, and the observer is obtained from the left coprimeness of the central controller; 3) the H parameter in the controller is used as a tradeoff between robust stability and performance.

II. Mathematical Model of the PMSM

The field orientation of the AC servo motor is defined as d-axis, and q-axis that leads the d-axis 90 electric degrees. In the d-q coordinates, the AC servo motor voltage-current and flux equations are shown as follows:

$$v_d = Ri_d + \dot{\lambda}_d - \omega_r \lambda_q \tag{1}$$

$$v_q = Ri_q + \dot{\lambda}_q - \omega_r \lambda_d \tag{2}$$

$$\lambda_d = L_d i_d + \lambda_{PM} \tag{3}$$

$$\lambda_q = L_q i_q \tag{4}$$

Where v_d and v_q are voltages of the d, q axis; R is the stator resistance; i_d and i_q are the d, q axis stator currents; ω_r is the rotor speed; λ_d and λ_q are the d, q axis flux induced by the currents of the d, q axis inductance; L_d and L_q are the q, d axis inductances with the same value, and λ_{PM} the constant mutual flux of the permanent magnet.

When the stator current vector is oriented perpendicular to the rotor magnetic field, the field-oriented control for Ac servo motor yields i_d =0. In the case, the electromagnetic torque is in strict positive proportion to i_q:

$$T_e = \frac{3P}{4} \cdot \lambda_{PM} \cdot i_q = K_T \cdot i_q \tag{5}$$

where P is the number of poles of motor, and K_T is the motor torque constant.

The mechanic motion equation is:

$$T_e = K_T i_q = T_d + B\omega_r + J\frac{d\omega_r}{dt} \tag{6}$$

where J is the moment of inertia; B is the viscous friction, and T_d is the torque disturbance such as the load resistance, the torque ripple and the resistance caused by nonlinear factors.

III. Design of the Control System

A. Control Scheme

978-0-7695-3272-1/08 $25.00 © 2008 IEEE
DOI 10.1109/LAB-RS.2008.27

The proposed control scheme is presented in Fig. 1 where the nominal plant is $G(s) = 1/(Js+B)$; K(s) is the velocity feedback controller designed by the loop shaping design procedure (LSDP) and the algebraic method, and the velocity lop controller is a servo controller. $K(s)$ is used for attenuating the disturbance T_L, and plant uncertainty, and the PDFF controller is used as velocity loop adjuster to improve the low-frequency stiffness.

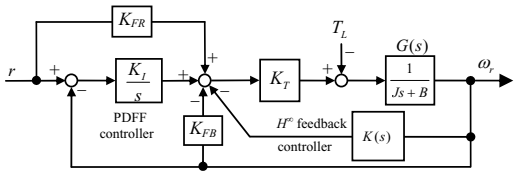

Fig. 1 Dual robust control scheme

B. Velocity Feedback Controller

In this paper, a continuous time control design approach based on H^∞-optimization control design is performed for a model of the AC servo system as seen from the digital computer control design approach. Consequently, performance is specified at the controller disturbance instants.

Minimum phase W_1 and W_2 are proper stable, real rational function denoted by RH^∞.The left and right coprime factorizations of W_1GW_2 are $\tilde{M}_S^{-1}\tilde{N}_S$ and $N_SM_S^{-1}$, respectively. Moreover, a doubly coprime factorization exists as follows:

$$\begin{bmatrix} X_r & Y_r \\ -\tilde{N}_S & \tilde{M}_S \end{bmatrix}\begin{bmatrix} M_S & -Y_l \\ N_S & X_l \end{bmatrix} = \begin{bmatrix} M_S & -Y_l \\ N_S & X_l \end{bmatrix}\begin{bmatrix} X_r & Y_r \\ -\tilde{N}_S & \tilde{M}_S \end{bmatrix} = I \tag{7}$$

where N_S, M_S, $\tilde{N}_S$, $\tilde{M}_S$, X_r, Y_r, X_l, and Y_l are over RH^∞. Then, the velocity controller $K(s)$ is defined as follows:

$$K(s) = W_1(s)K_v(s)W_2(s) \tag{8}$$

Where $K_v(s) = [X_r + H^{-1}Y_l\tilde{N}]^{-1}[Y_r - H^{-1}Y_l\tilde{M}]$ and H is a unit over RH^∞. With $K(s)$ of (8), the velocity feedback loop is internally stable. Moreover, X_r and Y_r of $K_v(s)$ in (8) play the similar role as central controller although H in $K_v(s)$ cannot be 0. According to this property, X_r and Y_r can be designed using the LSDP and H will be used to reject step and sinusoidal disturbance, as follows.

C. Design of Velocity Controller Using the LSDP and the Algebraic Method

The first stage in the LSDP uses a pre-matrix W_1 and/or a post-matrix W_2 to shape the singular values of the nominal plant G as a desired open-loop shape $G_S = W_2GW_1$. Constant or dynamic W_1 and W_2 are selected such that G_S has no hidden modes. Constant weighting matrices can improve the performance at low frequencies and increases the crossover frequency. Moreover, the dynamic W_1 or W_2 is used as the integral action with the phase-advance term for rejecting the input and output step disturbances. W_1 or W_2 is selected as the diagonal matrix and each principal element is $(s+\phi)/s$ where $\phi>0$ is lower than the crossover frequency. The integral action improves the performance at low frequencies, and the phase-advance term $s+\phi$ avoids the slope of the open-loop shaping at the crossover frequency more than –2, and adjusts the robustness in the feedback system. If ϕ is closer to the imaginary axis, the robustness is larger. The stage is the same as the velocity controller herein.

[11-14] advocate an expression of coprime factor uncertainty in terms of additive stable perturbations to coprime factors of the nominal plant. Such a class of perturbations has advantages over additive or multiplicative unstructured uncertainty model. For example, the number of unstable zeros and poles may change as the plant is perturbed. The perturbed plant [See Fig. 2.] is written

$$G_\Delta = (N_S + \Delta_N)\cdot(M_S + \Delta_M)^{-1} \tag{9}$$

where the pair (M_S, N_S) is a normalized right coprime factorization of G_S, and Δ_M and Δ_N are stable, unknown transfer functions representing the uncertainty and satisfying $\left\| \begin{bmatrix} \Delta_N \\ \Delta_M \end{bmatrix} \right\|_\infty < \varepsilon$, where $\varepsilon(>0)$ presents the stability margin.

In the second stage of the LSDP, the robust stabilization H^∞ problem is applied to the normalized right coprime factorization of G_S, and obtains a robust controller K_∞ satisfying

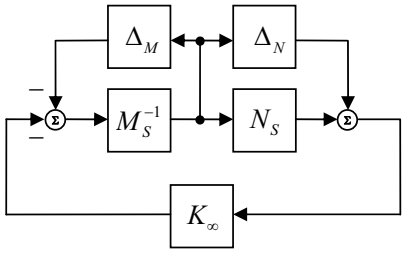

Fig. 2 Right coprime factor robust stabilization problem

$$\left\| M_S^{-1}(I + K_\infty G_S)^{-1}\begin{bmatrix} K_\infty & I \end{bmatrix} \right\|_\infty \le \varepsilon^{-1} \tag{10}$$

Suppose the shaped plant of G_S has the minimal realization (A, B, C, D). A central controller satisfying (10) is obtained as follows [15]:

$$K_\infty = \left[\begin{array}{c|c} A + BF + \gamma^2(W^T)^{-1}ZC^T(C+DF) & -\gamma^2(W^T)^{-1}ZC^T \\ \hline B^TX & D^T \end{array}\right] \tag{11}$$

where $F = -S^{-1}(D^TC + B^TX)$; $W = I + (XZ - \gamma^2 I)$, and X and Z are the solutions to the two algebraic Riccati equations as follows:

$$(A - BS^{-1}D^TC)^TX + X(A - BS^{-1}D^TC) - XBS^{-1}B^TX + C^TR^{-1}C = 0 \tag{12}$$

$$(A - BS^{-1}D^TC)Z + Z(A - BS^{-1}D^TC)^T - ZC^TR^{-1}CZ + BS^{-1}B^T = 0 \tag{13}$$

where $R = I+DD^T$, and $S = I+D^TD$.

If the plant is assumed to be strictly proper, i.e. $D = 0$, the realizations for the doubly coprime factorization can be presented as follows.

$$\begin{bmatrix} M_S \\ \hline N_S \end{bmatrix} = \left[\begin{array}{c|c} A + BF & B \\ \hline F & I \\ \hline C & 0 \end{array}\right] \tag{14}$$

$$\left[\tilde{N}_S \;\vdots\; \tilde{M}_S\right]=\left[\begin{array}{c|c:c} A+QLC & B & QL \\ \hline C & 0 & I \end{array}\right] \tag{15}$$

$$\left[X_r \;\vdots\; Y_r\right]=\left[\begin{array}{c|c:c} A+QLC & B & -QL \\ \hline -F & I & 0 \end{array}\right] \tag{16}$$

$$\left[X_l \;\vdots\; Y_l\right]=\left[\begin{array}{c|c:c} A+BF & B & -QL \\ \hline C & I & 0 \end{array}\right] \tag{17}$$

The pair $(\tilde{N}_S, \tilde{M}_S)$ in (15) is the left coprime factorization of G_S, but not the normalized left coprime factorization. Moreover, the pair (X_r, Y_r) are the left coprime factorization of K_∞ when $D = 0$. That is, $K_\infty = X_r^{-1} Y_r$. The result presents for the second stage of the velocity controller that the pair (X_r, Y_r) in $K_v(s)$ of (8) can be obtained from the left coprime factorization of K_∞ when $D = 0$.

In Fig. 1, the transfer function from T_L to ω_r is (18).

$$\omega_r = -W_1 N_S (X_r + H^{-1} Y_l \tilde{N}) W_1^{-1} \cdot T_L \tag{18}$$

For a step in T_L, ω_r with the zero steady state must satisfy the following equation, according to the final value theorem.

$$(X_r + H^{-1} Y_l \tilde{N}_S)\Big|_{s=0} = (H - M_S + X_r^{-1})\Big|_{s=0} = 0 \tag{19}$$

For rejecting a sinusoidal disturbance with known frequency σ in T_L, the following equation must be satisfied obviously.

$$(X_r + H^{-1} Y_l \tilde{N}_S)\Big|_{s=j\sigma} = (H - M_S + X_r^{-1})\Big|_{s=j\sigma} = 0 \tag{20}$$

Hence, for rejecting a step and/or sinusoidal disturbance in T_L, H can be designed algebraically. For example, if only the step disturbance exists in T_L, H is designed to be constant as follows.

$$H = (M_S - X_r^{-1})\Big|_{s=0} \tag{21}$$

If only a sinusoidal disturbance with known frequency σ_1 exists in T_L, H needs two unknown coefficients and is designed as follows:

$$H(s) = h_1 \frac{s + k_1}{s + p} \tag{22}$$

where H of (22) satisfies

$$H(s)\Big|_{s=j\sigma_1} = (M_S - X_r^{-1})\Big|_{s=j\sigma_1} \tag{23}$$

$p(>0)$ is given, and h_1 and k_1 can be solved according to (23). Analogously, if a number of n sinusoidal disturbances with n known frequencies $\sigma_1 \sim \sigma_n$, H needs $2n$ coefficients to be solved as follows.

$$H(s) = h_1 + \frac{h_2}{s+p} + \frac{h_3}{(s+p)^2} + \cdots + \frac{h_{2n}}{(s+p)^{2n-1}} \tag{24}$$

Hence, since the pair (X_r, Y_r) in K_v is the left coprime factorization of K_∞ in the LSDP, the completed velocity controller has several properties of the LSDP, including consideration of plant input and output performance, limited deteriorations at plant input and output, and bounded closed-loop objective functions. The three major properties of the LSDP are listed in [16]. Moreover, the velocity controller can use the H parameter to reject step and/or sinusoidal disturbances.

The velocity feedback loop also has robustness with coprime factor uncertainty, and satisfies the following robust inequality:

$$\left\| \begin{bmatrix} Y_r - H^{-1} Y_l \tilde{M}_S & X_r + H^{-1} Y_l \tilde{N}_S \end{bmatrix} \right\|_\infty \le \varepsilon_v^{-1} \tag{25}$$

where ε_v is the stability margin in the velocity feedback loop. Eq. (25) presents that the H parameter can affect the value of the stability margin ε_v. Herein, H is selected according to the control requirements and then the value of ε_v can be checked. H may need several redesigns to obtain a satisfactory value of ε_v. Moreover, for the sake of the numerical realization, K_v also can be written as $K_v = (1 + C_v X_r)^{-1} C_v Y_r$ where $C_v = H - M_S$.

D. PDFF Velocity Control Method

In digital control systems of AC servo drive, most of applications are using its velocity and torque control mode. The position loop of AC servo drive is taken control by outside multi-axis controller such as CNC controller. Many controllers design use PI velocity loops, eliminating the derivative term. Tuning PI loop is easy and is ideal for maximum responsiveness applications such as pick-and-place machines. But PI control has a weakness—because of its integral gain must remain relatively small to avoid excessive overshoot provides that it does not have good low frequency "stiffness". PDFF velocity control was developed to combat this problem. Fig. 3 shows the block diagram in frequency domain of a plant with a PDFF controller of the form:

$$u(s) = d(s) + K_{FR} \cdot r(s) + \frac{K_I}{s} \cdot e(s) - K_{FB} \cdot y(s) \tag{26}$$

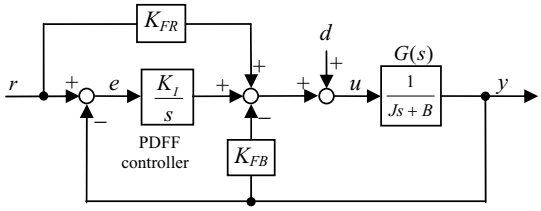

Fig. 3 Plant and disturbance with PDFF Controller

The transfer function of disturbance to output with the plant is simplified as a first order model is derived by

$$G_d(s) = \frac{s/J}{s^2 + \left(B/J + K_{FB}/J\right)s + K_I/J} = \frac{y(s)}{d(s)} \tag{27}$$

One of the most important specifications in many motion control applications is the load-torque disturbance rejection capability. The disturbance response can be tuned by moving closed poles more to the left side in the complex plane, and tracking response can be further optimized by adding zeros to the system via feedforward, as shown in (28).

$$G_c(s) = \frac{\left(K_I + K_{FR} s\right)/J}{s^2 + \left(B/J + K_{FB}/J\right)s + K_I/J} = \frac{y(s)}{r(s)} \tag{28}$$

The PDFF controller which locates the zero at an optimal place that shortens the step response rise time without overshoot.

IV. Results of Simulation Research

An high power AC servo motor model is included in the simulation, its mechanical parameters are: $J = 6.37$ and $B = 0.1$. According to the method discussed in part *C* of Section III, W_1, W_2, X_r, Y_r, H and C_v are given as follows.

$$W_1 = \frac{5\times10^3(s+2500)}{s},\ W_2 = 1,$$

$$X_r = \frac{s^2+1.395\times10^4 s+2.348\times10^7}{s^2+1.181\times10^4 s+1.216\times10^7},$$

$$Y_r = \frac{2.016\times10^4 s+1.216\times10^7}{s^2+1.181\times10^4 s+1.216\times10^7}$$

$$H = \frac{-0.393(s+2.713\times10^3)}{s+1}$$

$$C_v = \frac{-1.393s^3-1.903\times10^3 s^2-3.040\times10^6 s-2.090\times10^9}{s^3+2.132\times10^3 s^2+1.965\times10^6 s+1.962\times10^6}$$

The Simulink model of the velocity control loop with PDFF and H^∞ feedback controller is shown is Fig. 3. The comparison on the simulation results of the velocity control loop with PI and PDFF plus H^∞ feedback controller is indicated in Fig. 4(d) shown the response of the two types of controller when the step and sine disturbance is added to the system.

The design yields that G_S has the crossover frequency about 300Hz as shown in Fig. 4(a), and the velocity feedback loop have the stability margin 19.36%. Moreover, it yields that the velocity feedback loop can reject the 250Nm step at 0.02 sec and 300Hz sinusoidal at 0 sec disturbances in T_L as shown in Fig. 4(b), and the input sensitivity, $W_1M_SX_rW_1^{-1}$ is presented in Fig. 4(c). The effect of PDFF controller also has contribution on the disturbance rejection, as shown in Fig. 4(b).

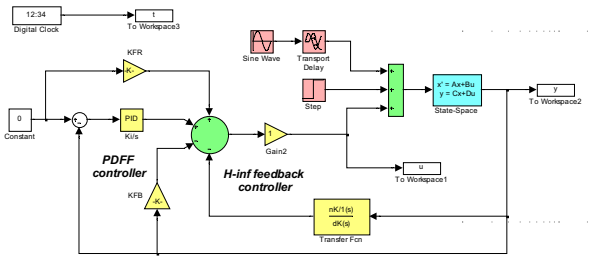

Fig. 3. Simulink model of PDFF plus H^∞ feedback controller

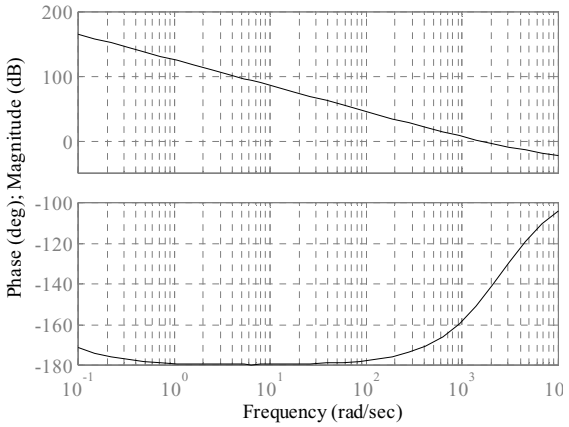

(a) Bode plot of *Gs*

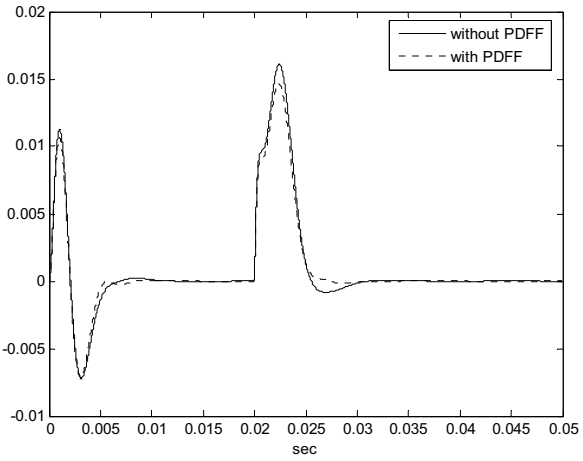

(b)

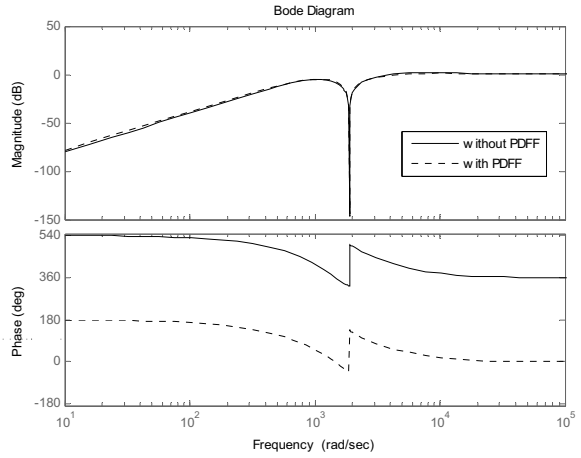

(c)

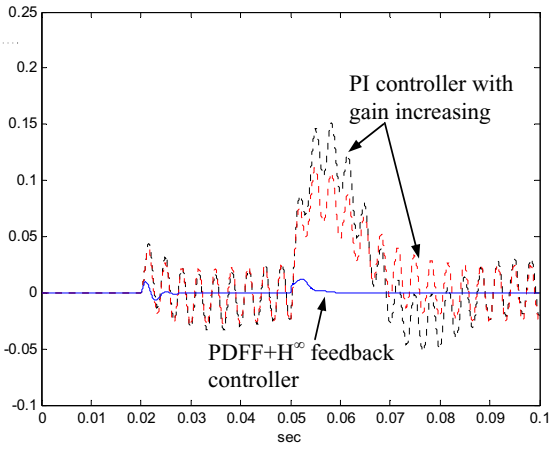

(d) Disturbance responses comparison of PI and dual robust controller

Fig. 4 (a) G_S shape (b) disturbance responses with 250Nm step (at 0.02sec) and sin600πt (at 0 sec) (c) input sensitivity (d) Disturbance responses comparison of PI and dual robust controller with 250Nm step (at 0.05sec) and sin600πt (at 0.02 sec)

In digital systems, many manufacturers use PI velocity loops, eliminating the derivative term. PI loops are easy to tuneand is ideal for applications that demand the maximum responsiveness such as pick-and-place machines. But PI

control has a weakness—it does not provide good low frequency "stiffness". The key difference between PI and PDFF is that PDFF forces the entire error signal through integration. This makes PDFF less responsive to the velocity command than PI. Although the feed-forward term injects the command ahead of the integral making the system more responsive to commands, moving average (MA) filter of error signal is considered to improve the system responsiveness. Fig. 6 shows the step response of a AC servo motor and drive system with MA filter compensation in the velocity loop. Figure 6(a)(b) shown that MA compensation can improve the system response while in the heavy load driving period.

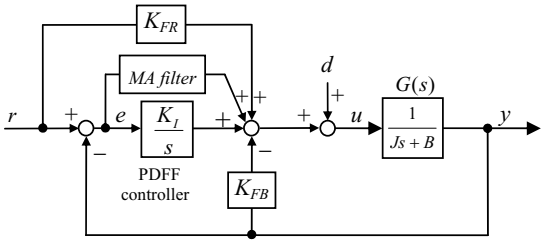

Fig. 5 Block diagram of PDFF controller with MA filter.

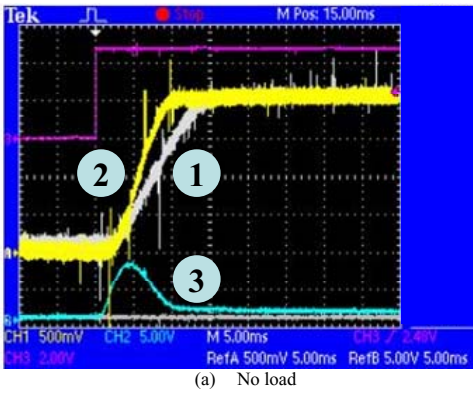

(a) No load

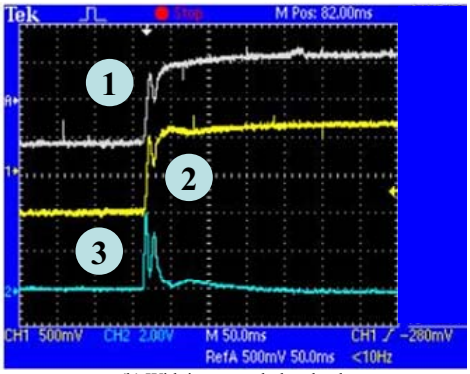

(b) With iron round plate load

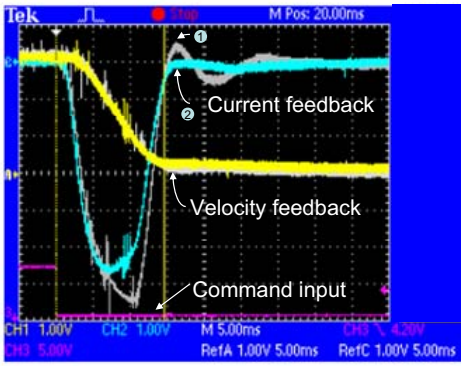

(c) Velocity feedback and Current feedback response

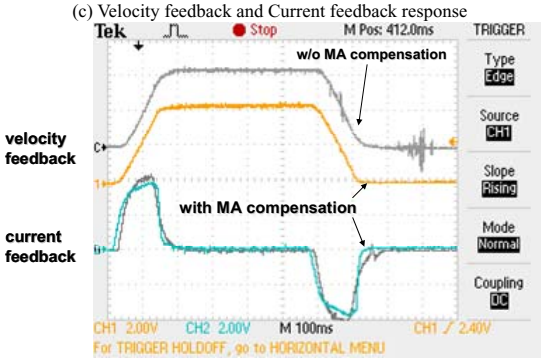

(d) Velocity feedback and Current feedback response

Fig. 6 AC servo drive step response: (a) no load (b) with load. (c)(d) These comparisons are using the same set of parameters, new program has better response and less overshoot. ❶w/o compensation, ❷with compensation, ❸MA compensation signal.

V. Conclusions

This paper proposes a dual robust controller design for the velocity loop of a high performance AC servo motor speed servo using PDFF-MA and H^{∞} feedback control to meet the requirements of robust stability, exterior load disturbances rejection, low-frequency stiffness and responsiveness. The simulation and experimental results demonstrate the good control performance of the proposed control scheme.

Acknowledgment

Research supported by MSL project, ITRI, Taiwan, ROC.
Corresponding author E-mail: stonecheng@mail.nctu.edu.tw

References

[1] W. Leonhard, "Microcomputer Control of High Dynamic Performance ac=drives-A survey" Automatica, Vol.22, No.1, pp.1-19, 1986.

[2] T.-L. Hsien, Y.-Y. Sun, M.-C. Tsai, "H^{∞} control for a sensorless permanent-magnet synchronous drive" *IEE Proc-Electr. Power Appl., Vol. 144, No.3, May 1997,* pp. 173-181

[3] Xie Dongmei, Qu Daokui, Xu Fang, "Design of H_{∞} Feedback Controller and IP-Position Controller of PMSM Servo System" Proceedings of the IEEE International Conference on Mechatronics & Automation Niagara Falls, Canada, July 2005

[4] Jong-Sun Ko, Hyunsik Kim, and Seong-Hyun Yang, "Precision Speed Control of PMSM Using Neural Network Disturbance Observer on Forced Nominal Plant", Proceedings of the 5th Asian Control Conference, July 2004

[5] Tom Oomen, Marc van de Wal, and Okko Bosgra, "Exploiting H∞ Sampled-Data Control Theory for High-Precision Electromechanical Servo Control Design", Proceedings of the 2006 American Control Conference, June, 2006

[6] Pragasen Pillay, Ramu Krishnan "Control Characteristic and Speed Controller Design for a High Performance Permanent Magnet Synchronous Motor Drive" *IEEE Trans. Power Elec..*, vol. 5, No. 2, April

1990, pp. 151-159.
[7] S.M. Zeid, T.S. Radwan and M.A. Rahman, “Real-Time Implementation of Multiple feedback loop control for a Permanent Magnet Synchronous Motor Drive” *IEEE Proc .Canadian Conf on Elec. And Comp. End.*. pp. 1265-1270, 1999.
[8] Wenhuo Zeng and Jun Hu, “Application of Intelligent PDF Control Algorithm to an Electrohydraulic Position Servo System” Proc. Of the 1999 *IEEE/ASME, Int. Conf. on Advanced Intelligent Mechatronics.* pp. 233-238.
[9] Z Nagy and A Bradshaw “Comparison of PI and PDF controls of a Manipulator ARM” *UKACC Int. Conf. on Control ‘98*, pp. 739-744.
[10] Ali Saberi, Anton A. Stoorvogel, Peddapullaiah Sannuti, “Analysis, design, and performance limitations of H∞ optimal filtering in the presence of an additional input with known frequency”, Proceedings of the 2006 American Control Conference, June, 2006
[11] M. Vidyasagar, *Control System Synthesis: A Coprime Factorization Approach*. Cambridge, MA: M.I.T. Press, 1985.
[12] M. Vidyasagar, “The graph metric for unstable plants and robustness estimates for feedback stability,” *IEEE Trans. Automat. Contr.*, vol. 39, pp. 403-417, 1984.
[13] M. Vidyasagar and H. Kumira, “Robust controllers for uncertain linear multivariable systems,” *Automatica*, pp. 85-94, 1986.
[14] T. T. Georgiou and M. C. Smith, “Optimal robustness in the gap metric,” *IEEE Trans. Automat. Contr.*, vol. 35, pp. 673-686, June 1990.
[15] K. Glover and D. McFarlane, “Robust stabilization of normalized coprime factor plant descriptions with H_∞-bounded uncertainty,” *IEEE Trans. Automat. Contr.*, vol. 34, pp. 821-830, Aug. 1989.
[16] D. McFarlane and K. Glover, “A loop shaping design procedure using H_∞ synthesis,” *IEEE Trans. Automat. Contr.*, vol. 37, no. 6, pp. 759-769, June 1992.